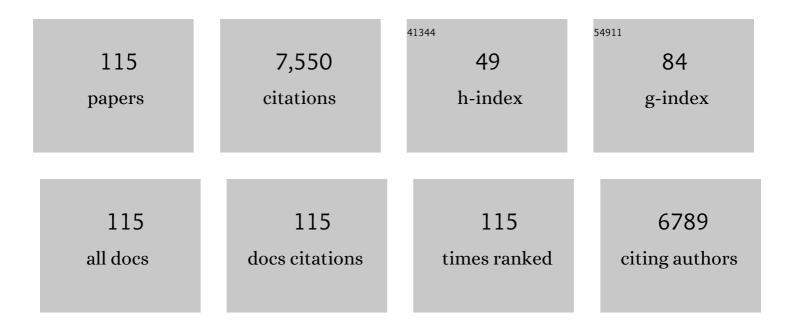
List of Publications by Year in descending order

Source: https://exaly.com/author-pdf/2280963/publications.pdf Version: 2024-02-01



ΡΑΝΙ Κ ΚΙΙΚΚΑΠΑΒΙΙ

#	Article	IF	CITATIONS
1	Secondary mineralization pathways induced by dissimilatory iron reduction of ferrihydrite under advective flow. Geochimica Et Cosmochimica Acta, 2003, 67, 2977-2992.	3.9	561
2	Synthesis of Colloidal Mn2+:ZnO Quantum Dots and High-TCFerromagnetic Nanocrystalline Thin Films. Journal of the American Chemical Society, 2004, 126, 9387-9398.	13.7	394
3	Biomineralization of Poorly Crystalline Fe(III) Oxides by Dissimilatory Metal Reducing Bacteria (DMRB). Geomicrobiology Journal, 2002, 19, 179-207.	2.0	349
4	Anaerobic redox cycling of iron by freshwater sediment microorganisms. Environmental Microbiology, 2006, 8, 100-113.	3.8	290
5	Influence of Coprecipitated Organic Matter on Fe <sup>2+</sup> <sub>(aq)</sub> -Catalyzed Transformation of Ferrihydrite: Implications for Carbon Dynamics. Environmental Science & Technology, 2015, 49, 10927-10936.	10.0	192
6	Reduction of TcO4â^' by sediment-associated biogenic Fe(II). Geochimica Et Cosmochimica Acta, 2004, 68, 3171-3187.	3.9	184
7	Mineral transformations associated with the microbial reduction of magnetite. Chemical Geology, 2000, 169, 299-318.	3.3	180
8	Biotransformation of two-line silica-ferrihydrite by a dissimilatory Fe(III)-reducing bacterium: formation of carbonate green rust in the presence of phosphate. Geochimica Et Cosmochimica Acta, 2004, 68, 2799-2814.	3.9	164
9	Reductive Sequestration of Pertechnetate ( <sup>99</sup> TcO <sub>4</sub> <sup>–</sup> ) by Nano Zerovalent Iron (nZVI) Transformed by Abiotic Sulfide. Environmental Science & Technology, 2013, 47, 5302-5310.	10.0	162
10	Phosphate Imposed Limitations on Biological Reduction and Alteration of Ferrihydrite. Environmental Science & Technology, 2007, 41, 166-172.	10.0	160
11	Reduction of pertechnetate [Tc(VII)] by aqueous Fe(II) and the nature of solid phase redox products. Geochimica Et Cosmochimica Acta, 2007, 71, 2137-2157.	3.9	154
12	Control of Fe(III) site occupancy on the rate and extent of microbial reduction of Fe(III) in nontronite. Geochimica Et Cosmochimica Acta, 2005, 69, 5429-5440.	3.9	142
13	Reduction of Hg(II) to Hg(0) by Magnetite. Environmental Science & Technology, 2009, 43, 5307-5313.	10.0	138
14	Microbial Reduction of Structural Fe(III) in Illite and Goethite. Environmental Science & Technology, 2003, 37, 1268-1276.	10.0	128
15	Bioreduction of Fe-bearing clay minerals and their reactivity toward pertechnetate (Tc-99). Geochimica Et Cosmochimica Acta, 2011, 75, 5229-5246.	3.9	128
16	Iron Loading Effects in Fe/SSZ-13 NH <sub>3</sub> -SCR Catalysts: Nature of the Fe Ions and Structure–Function Relationships. ACS Catalysis, 2016, 6, 2939-2954.	11.2	126
17	Adsorption of phenol and chlorinated phenols from aqueous solution by tetramethylammonium- and tetramethylphosphonium-exchanged montmorillonite. Applied Clay Science, 1998, 13, 13-20.	5.2	119
18	Organic Matter Remineralization Predominates Phosphorus Cycling in the Mid-Bay Sediments in the Chesapeake Bay. Environmental Science & Technology, 2015, 49, 5887-5896.	10.0	117

#	Article	IF	CITATIONS
19	Transformation of 2-line ferrihydrite to 6-line ferrihydrite under oxic and anoxic conditions. American Mineralogist, 2003, 88, 1903-1914.	1.9	114
20	Long-term dynamics of uranium reduction/reoxidation under low sulfate conditions. Geochimica Et Cosmochimica Acta, 2008, 72, 3603-3615.	3.9	111
21	Biological Redox Cycling of Iron in Nontronite and Its Potential Application in Nitrate Removal. Environmental Science & Technology, 2015, 49, 5493-5501.	10.0	109
22	Fe/SSZ-13 as an NH3-SCR catalyst: A reaction kinetics and FTIR/Mössbauer spectroscopic study. Applied Catalysis B: Environmental, 2015, 164, 407-419.	20.2	108
23	Abiotic Reductive Immobilization of U(VI) by Biogenic Mackinawite. Environmental Science & Technology, 2013, 47, 2361-2369.	10.0	100
24	Dissimilatory bacterial reduction of Al-substituted goethite in subsurface sediments. Geochimica Et Cosmochimica Acta, 2001, 65, 2913-2924.	3.9	98
25	Redox Fluctuations Control the Coupled Cycling of Iron and Carbon in Tropical Forest Soils. Environmental Science & Technology, 2018, 52, 14129-14139.	10.0	96
26	Microbial Lithotrophic Oxidation of Structural Fe(II) in Biotite. Applied and Environmental Microbiology, 2012, 78, 5746-5752.	3.1	94
27	Transformation of Active Sites in Fe/SSZ-13 SCR Catalysts during Hydrothermal Aging: A Spectroscopic, Microscopic, and Kinetics Study. ACS Catalysis, 2017, 7, 2458-2470.	11.2	89
28	Biological oxidation of Fe(II) in reduced nontronite coupled with nitrate reduction by Pseudogulbenkiania sp. Strain 2002. Geochimica Et Cosmochimica Acta, 2013, 119, 231-247.	3.9	88
29	Uranium in Framboidal Pyrite from a Naturally Bioreduced Alluvial Sediment. Environmental Science & Technology, 2009, 43, 8528-8534.	10.0	85
30	Fractionation of oxygen isotopes in phosphate during its interactions with iron oxides. Geochimica Et Cosmochimica Acta, 2010, 74, 1309-1319.	3.9	85
31	Tetramethylphosphonium- and Tetramethylammonium-Smectites as Adsorbents of Aromatic and Chlorinated Hydrocarbons: Effect of Water on Adsorption Efficiency. Clays and Clay Minerals, 1995, 43, 318-323.	1.3	84
32	Biotransformation of Ni-Substituted Hydrous Ferric Oxide by an Fe(III)-Reducing Bacterium. Environmental Science & Technology, 2001, 35, 703-712.	10.0	83
33	Synthesis and properties of titanomagnetite (Fe3â^'xTixO4) nanoparticles: A tunable solid-state Fe(II/III) redox system. Journal of Colloid and Interface Science, 2012, 387, 24-38.	9.4	80
34	Catalytic N2O decomposition and reduction by NH3 over Fe/Beta and Fe/SSZ-13 catalysts. Journal of Catalysis, 2018, 358, 199-210.	6.2	80
35	Copper Sorption Mechanisms on Smectites. Clays and Clay Minerals, 2004, 52, 321-333.	1.3	78
36	Ferrous hydroxy carbonate is a stable transformation product of biogenic magnetite. American Mineralogist, 2005, 90, 510-515.	1.9	75

#	Article	IF	CITATIONS
37	Effects of redox cycling of iron in nontronite on reduction of technetium. Chemical Geology, 2012, 291, 206-216.	3.3	75
38	Oxidative Remobilization of Technetium Sequestered by Sulfide-Transformed Nano Zerovalent Iron. Environmental Science & Technology, 2014, 48, 7409-7417.	10.0	73
39	Microbial and Mineralogical Characterizations of Soils Collected from the Deep Biosphere of the Former Homestake Gold Mine, South Dakota. Microbial Ecology, 2010, 60, 539-550.	2.8	70
40	Influence of electron donor/acceptor concentrations on hydrous ferric oxide (HFO) bioreduction. Biodegradation, 2003, 14, 91-103.	3.0	69
41	Reduction of Tc(VII) by Fe(II) Sorbed on Al (hydr)oxides. Environmental Science & Technology, 2008, 42, 5499-5506.	10.0	69
42	Reductive biotransformation of Fe in shale–limestone saprolite containing Fe(III) oxides and Fe(II)/Fe(III) phyllosilicates. Geochimica Et Cosmochimica Acta, 2006, 70, 3662-3676.	3.9	67
43	Biotic and Abiotic Pathways of Phosphorus Cycling in Minerals and Sediments: Insights from Oxygen Isotope Ratios in Phosphate. Environmental Science & Technology, 2011, 45, 6254-6261.	10.0	66
44	Kinetics and Mechanism of Birnessite Reduction by Catechol. Soil Science Society of America Journal, 2001, 65, 58-66.	2.2	61
45	Oxidative dissolution of UO2 in a simulated groundwater containing synthetic nanocrystalline mackinawite. Geochimica Et Cosmochimica Acta, 2013, 102, 175-190.	3.9	61
46	Biostimulation of iron reduction and subsequent oxidation of sediment containing Fe-silicates and Fe-oxides: Effect of redox cycling on Fe(III) bioreduction. Water Research, 2007, 41, 2996-3004.	11.3	60
47	Solid-Phase Fe Speciation along the Vertical Redox Gradients in Floodplains using XAS and Mössbauer Spectroscopies. Environmental Science & Technology, 2017, 51, 7903-7912.	10.0	58
48	Redoxâ€Active Metal–Organic Composites for Highly Selective Oxygen Separation Applications. Advanced Materials, 2016, 28, 3572-3577.	21.0	55
49	Cerium Substitution in Yttrium Iron Garnet: Valence State, Structure, and Energetics. Chemistry of Materials, 2014, 26, 1133-1143.	6.7	53
50	Microbial reduction of fe(III) in the Fithian and Muloorina illites: contrasting extents and rates of bioreduction. Clays and Clay Minerals, 2006, 54, 67-79.	1.3	51
51	Biogeochemical transformation of Fe minerals in a petroleum-contaminated aquifer. Geochimica Et Cosmochimica Acta, 2004, 68, 1791-1805.	3.9	49
52	Biogeochemical Processes In Ethanol Stimulated Uranium-contaminated Subsurface Sediments. Environmental Science & Technology, 2008, 42, 4384-4390.	10.0	49
53	Reduced Magnetism in Core–Shell Magnetite@MOF Composites. Nano Letters, 2017, 17, 6968-6973.	9.1	47
54	Iron oxide waste form for stabilizing 99Tc. Journal of Nuclear Materials, 2012, 429, 201-209.	2.7	46

4

**ΓΑνι Κ Κυκκαdapu** 

#	Article	IF	CITATIONS
55	Microbial reduction of uranium under iron- and sulfate-reducing conditions: Effect of amended goethite on microbial community composition and dynamics. Water Research, 2010, 44, 4015-4028.	11.3	45
56	Abiotic U(VI) reduction by sorbed Fe(II) on natural sediments. Geochimica Et Cosmochimica Acta, 2013, 117, 266-282.	3.9	43
57	Nepheline crystallization in boron-rich alumino-silicate glasses as investigated by multi-nuclear NMR, Raman, & Mössbauer spectroscopies. Journal of Non-Crystalline Solids, 2015, 409, 149-165.	3.1	42
58	Effects of sediment iron mineral composition on microbially mediated changes in divalent metal speciation: Importance of ferrihydrite. Geochimica Et Cosmochimica Acta, 2005, 69, 1739-1754.	3.9	41
59	Structure and thermodynamics of uranium-containing iron garnets. Geochimica Et Cosmochimica Acta, 2016, 189, 269-281.	3.9	41
60	Geochemical and mineralogical investigation of uranium in multi-element contaminated, organic-rich subsurface sediment. Applied Geochemistry, 2014, 42, 77-85.	3.0	40
61	Microbial Reductive Transformation of Phyllosilicate Fe(III) and U(VI) in Fluvial Subsurface Sediments. Environmental Science & Technology, 2012, 46, 3721-3730.	10.0	34
62	Identifying sources and cycling of phosphorus in the sediment of a shallow freshwater lake in China using phosphate oxygen isotopes. Science of the Total Environment, 2019, 676, 823-833.	8.0	34
63	The mineralogic transformation of ferrihydrite induced by heterogeneous reaction with bioreduced anthraquinone disulfonate (AQDS) and the role of phosphate. Geochimica Et Cosmochimica Acta, 2011, 75, 6330-6349.	3.9	33
64	Iron and Arsenic Speciation During As(III) Oxidation by Manganese Oxides in the Presence of Fe(II): Molecular-Level Characterization Using XAFS, MA¶ssbauer, and TEM Analysis. ACS Earth and Space Chemistry, 2018, 2, 256-268.	2.7	32
65	Uranium storage mechanisms in wet-dry redox cycled sediments. Water Research, 2019, 152, 251-263.	11.3	32
66	Synthesis and electron spin resonance studies of copper-doped alumina-pillared montmorillonite clay. The Journal of Physical Chemistry, 1988, 92, 6073-6078.	2.9	31
67	Synthesis of a Low-Carbonate High-Charge Hydrotalcite-like Compound at Ambient Pressure and Atmosphere. Chemistry of Materials, 1997, 9, 417-419.	6.7	30
68	Mössbauer and optical spectroscopic study of temperature and redox effects on iron local environments in a Fe-doped (0.5 mol% Fe2O3) 18Na2O–72SiO2 glass. Journal of Non-Crystalline Solids, 2003, 317, 301-318.	3.1	30
69	Biomineralization associated with microbial reduction of Fe3+ and oxidation of Fe2+ in solid minerals. American Mineralogist, 2009, 94, 1049-1058.	1.9	30
70	Charge-Coupled Substituted Garnets (Y <sub>3–<i>x</i></sub> Ca <sub>0.5<i>x</i></sub> M <sub>0.5<i>x</i></sub> )Fe <sub>5</sub> O <sub>12(M = Ce, Th): Structure and Stability as Crystalline Nuclear Waste Forms. Inorganic Chemistry, 2015, 54, 4156-4166.</sub>	ub> 4.0	29
71	Root-driven weathering impacts on mineral-organic associations in deep soils over pedogenic time scales. Geochimica Et Cosmochimica Acta, 2019, 263, 68-84.	3.9	29
72	Strong mineralogic control of soil organic matter composition in response to nutrient addition across diverse grassland sites. Science of the Total Environment, 2020, 736, 137839.	8.0	29

**ΓΑνι Κ Κυκκαdapu** 

#	Article	IF	CITATIONS
73	Fe(II) sorption on pyrophyllite: Effect of structural Fe(III) (impurity) in pyrophyllite on nature of layered double hydroxide (LDH) secondary mineral formation. Chemical Geology, 2016, 439, 152-160.	3.3	28
74	Lignin-enhanced reduction of structural Fe(III) in nontronite: Dual roles of lignin as electron shuttle and donor. Geochimica Et Cosmochimica Acta, 2021, 307, 1-21.	3.9	27
75	Uranium Extraction From Laboratory-Synthesized, Uranium-Doped Hydrous Ferric Oxides. Environmental Science & Technology, 2009, 43, 2341-2347.	10.0	26
76	Mobilization of metals from Eau Claire siltstone and the impact of oxygen under geological carbon dioxide sequestration conditions. Geochimica Et Cosmochimica Acta, 2014, 141, 62-82.	3.9	25
77	Electron transfer between sorbed Fe(II) and structural Fe(III) in smectites and its effect on nitrate-dependent iron oxidation by Pseudogulbenkiania sp. strain 2002. Geochimica Et Cosmochimica Acta, 2019, 265, 132-147.	3.9	23
78	Changes in Sedimentary Phosphorus Burial Following Artificial Eutrophication of Lake 227, Experimental Lakes Area, Ontario, Canada. Journal of Geophysical Research G: Biogeosciences, 2020, 125, e2020JG005713.	3.0	23
79	Isolation and Microbial Reduction of Fe(III) Phyllosilicates from Subsurface Sediments. Environmental Science & Technology, 2012, 46, 11618-11626.	10.0	21
80	Iron mineralogy and uranium-binding environment in the rhizosphere of a wetland soil. Science of the Total Environment, 2016, 569-570, 53-64.	8.0	21
81	"Switching on―iron in clay minerals. Environmental Science: Nano, 2019, 6, 1704-1715.	4.3	21
82	Physical and electrical properties of melt-spun Fe-Si (3–8 wt.%) soft magnetic ribbons. Materials Characterization, 2018, 136, 212-220.	4.4	20
83	Synthesis of nanometer-sized fayalite and magnesium-iron(II) mixture olivines. Journal of Colloid and Interface Science, 2018, 515, 129-138.	9.4	19
84	Role of clay-associated humic substances in catalyzing bioreduction of structural Fe(III) in nontronite by Shewanella putrefaciens CN32. Science of the Total Environment, 2020, 741, 140213.	8.0	19
85	Efficacy of acetate-amended biostimulation for uranium sequestration: Combined analysis of sediment/groundwater geochemistry and bacterial community structure. Applied Geochemistry, 2017, 78, 172-185.	3.0	18
86	Technetium and iodine aqueous species immobilization and transformations in the presence of strong reductants and calcite-forming solutions: Remedial action implications. Science of the Total Environment, 2018, 636, 588-595.	8.0	17
87	2H Solid-State NMR Investigation of Terephthalate Dynamics and Orientation in Mixed-Anion Hydrotalcite-Like Compounds. Journal of Physical Chemistry B, 1999, 103, 5197-5203.	2.6	16
88	<sup>99</sup> Tc(VII) Retardation, Reduction, and Redox Rate Scaling in Naturally Reduced Sediments. Environmental Science & Technology, 2015, 49, 13403-13412.	10.0	15
89	Interactions Between Fe(III)-oxides and Fe(III)-phyllosilicates During Microbial Reduction 2: Natural Subsurface Sediments. Geomicrobiology Journal, 2017, 34, 231-241.	2.0	14
90	Calcareous organic matter coatings sequester siderophores in alkaline soils. Science of the Total Environment, 2020, 724, 138250.	8.0	14

**ΓΑνι Κ Κυκκαdapu** 

#	Article	IF	CITATIONS
91	Syntrophic Effects in a Subsurface Clostridial Consortium on Fe(III)-(Oxyhydr)oxide Reduction and Secondary Mineralization. Geomicrobiology Journal, 2014, 31, 101-115.	2.0	13
92	Electron spin resonance and X-ray diffraction studies of copper(II)-ion-doped Zr4-pillared montmorillonite clay. Journal of the Chemical Society, Faraday Transactions, 1990, 86, 691.	1.7	11
93	Anomalous water expulsion from carbon-based rods at high humidity. Nature Nanotechnology, 2016, 11, 791-797.	31.5	11
94	Susceptibility of new soil organic carbon to mineralization during dry-wet cycling in soils from contrasting ends of a precipitation gradient. Soil Biology and Biochemistry, 2022, 169, 108681.	8.8	11
95	Bioavailability of Fe(III) In Loess Sediments: An Important Source of Electron Acceptors. Clays and Clay Minerals, 2010, 58, 542-557.	1.3	10
96	Uranium fate in Hanford sediment altered by simulated acid waste solutions. Applied Geochemistry, 2015, 63, 1-9.	3.0	9
97	A study of the corrosion products of mild steel in high ionic strength brines. Waste Management, 2001, 21, 335-341.	7.4	8
98	Mössbauer Spectral Properties of Yttrium Iron Garnet, Y <sub>3</sub> Fe <sub>5</sub> O <sub>12</sub> , and Its Isovalent and Nonisovalent Yttrium-Substituted Solid Solutions. Inorganic Chemistry, 2016, 55, 3413-3418.	4.0	8
99	Spontaneous redox continuum reveals sequestered technetium clusters and retarded mineral transformation of iron. Communications Chemistry, 2020, 3, .	4.5	8
100	Studies of the oxidation state and location of palladium species in Al13-pillared montmorillonite. Journal of the Chemical Society, Faraday Transactions, 1991, 87, 3083.	1.7	7
101	Interactions Between Fe(III)-Oxides and Fe(III)-Phyllosilicates During Microbial Reduction 1: Synthetic Sediments. Geomicrobiology Journal, 2016, 33, 793-806.	2.0	7
102	Switchable Ionic Liquids: An Environmentally Friendly Medium to Synthesise Nanoparticulate Green Rust. Current Inorganic Chemistry, 2016, 6, 92-99.	0.2	6
103	Size effects on gamma radiation response of magnetic properties of barium hexaferrite powders. Journal of Applied Physics, 2011, 110, .	2.5	5
104	Fast redox switches lead to rapid transformation of goethite in humid tropical soils: A Mössbauer spectroscopy study. Soil Science Society of America Journal, 2022, 86, 264-274.	2.2	4
105	Selective Interactions of Soil Organic Matter Compounds with Calcite and the Role of Aqueous Ca. ACS Earth and Space Chemistry, 0, , .	2.7	4
106	Tetragonal-Like Phase in Core–Shell Iron Iron-Oxide Nanoclusters. Journal of Physical Chemistry C, 2017, 121, 11794-11803.	3.1	3
107	Dispersible Colloid Facilitated Release of Organic Carbon From Two Contrasting Riparian Sediments. Frontiers in Water, 2020, 2, .	2.3	3
108	Waterâ€dispersible nanocolloids and higher temperatures promote the release of carbon from riparian soil. Vadose Zone Journal, 2020, 19, e20077.	2.2	2

#	Article	IF	CITATIONS
109	Elemental iron: reduction of pertechnetate in the presence of silica and periodicity of precipitated nano-structures. Environmental Science: Nano, 2021, 8, 97-109.	4.3	2
110	Strong Purcell enhancement at telecom wavelengths afforded by spinel Fe3O4 nanocrystals with size-tunable plasmonic properties. Nanoscale Horizons, 2021, , .	8.0	2
111	The solubility of 242PuO2 in the presence of aqueous Fe(II): the impact of precipitate preparation. Radiochimica Acta, 2014, 102, 861.	1.2	0
112	Macro to Nanoscale Approaches to Study Mineral Transformations at the Liquid, Organic, Biological Interface Microscopy and Microanalysis, 2020, 26, 1568-1569.	0.4	0
113	Characterizing the localization of organic C on mineral surfaces: a correlative microscopy/spectroscopy approach. Microscopy and Microanalysis, 2021, 27, 306-307.	0.4	0
114	Stability of mineralâ€organic matter associations under varying biogeochemical conditions. Soil Science Society of America Journal, 0, , .	2.2	0
115	SSSAJ 2021 Publisher's Report. Soil Science Society of America Journal, 2022, 86, 868-878.	2.2	Ο